Inorganic Chemistry

Article

pubs.acs.org/IC

Evaluation of Donor and Steric Properties of Anionic Ligands on High Valent Transition Metals

Stephen A. DiFranco, Nicholas A. Maciulis, Richard J. Staples, Rami J. Batrice, and Aaron L. Odom*

Department of Chemistry, Michigan State University, East Lansing, Michigan 48824, United States

Supporting Information

ABSTRACT: Synthetic protocols and characterization data for a variety of chromium(VI) nitrido compounds of the general formula $NCr(NPr^i_2)_2X$ are reported, where X = NPr^i_2 (**1**), I (**2**), Cl (**3**), Br (**4**), OTf (**5**), 1-adamantoxide (**6**), $OSiPh_3$ (**7**), O_2CPh (**8**), OBu^t_{F6} (**9**), OPh (**10**), O-*p*-$(OMe)C_6H_4$ (**11**), O-*p*-$(SMe)C_6H_4$ (**12**), O-*p*-$(Bu^t)C_6H_4$ (**13**), O-*p*-$(F)C_6H_4$ (**14**), O-*p*-$(Cl)C_6H_4$ (**15**), O-*p*-$(CF_3)C_6H_4$ (**16**), OC_6F_5 (**17**), κ(O)-*N*-oxy-phthalimide (**18**), SPh (**19**), OCH_2Ph (**20**), NO_3 (**21**), pyrrolyl (**22**), 3-C_6F_5-pyrrolyl (**23**), 3-$[3,5\text{-}(CF_3)_2C_6H_3]$pyrrolyl (**24**), indolyl (**25**), carbazolyl (**26**), N(Me)Ph (**27**), κ(N)-NCO (**28**), κ(N)-NCS (**29**), CN (**30**), NMe_2 (**31**), F (**33**). Several different techniques were employed in the syntheses, including nitrogen-atom transfer for the formation of **1**. A cationic chromium complex $[NCr(NPr^i_2)_2(DMAP)]BF_4$ (**32**) was used as an intermediate for the production of **33**, which was produced by tin-catalyzed degredation of the salt. Using spin saturation transfer or line shape analysis, the free energy barriers for diisopropylamido rotation were studied. It is proposed that the estimated enthalpic barriers, Ligand Donor Parameters (LDPs), for amido rotation can be used to parametrize the donor abilities of this diverse set of anionic ligands toward transition metal centers in low d-electron counts. The new LDPs do not correlate well to the pK_a value of X. Conversely, the LDP values of phenoxide ligands do correlate with Hammett parameters for the *para*-substituents. Literature data for ^{13}C NMR chemical shifts for a tungsten-based system with various X ligands plotted versus LDP provided a linear fit. In addition, the angular overlap model derived $e_\sigma + e_\pi$ values for chromium(III) ammine complexes correlate with LDP values. Also discussed is the correlation with $XTiCp^*_2$ spectroscopic data. X-ray diffraction has been used used to characterize 31 of the compounds. From the X-ray diffraction data, steric parameters for the ligands using the Percent Buried Volume and Solid Angle techniques were found.

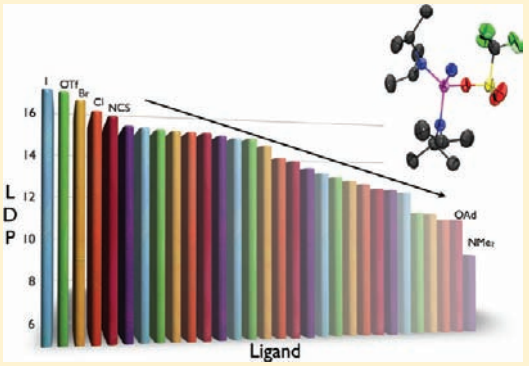

INTRODUCTION

One of the most important methods for controlling reaction pathways in many transition metal catalyzed systems is through the steric and electronic adjustment of ancillary ligands. Choosing from the extensive gallery of possible ligand choices is often done by (1) analogy with similar reactions already in the literature, (2) picking readily available ancillaries in the investigator's laboratory, or (3) making an educated guess based on experience in the field. Once some of the desired reactivity is found, reactions are optimized through similar procedures involving available ligand sets and trying to encourage hypothesized processes with slow reaction rates. Finally, a reaction may be deemed interesting enough to warrant full mechanistic investigations through experimental and computational techniques that can often lead to improved catalyst designs.

In this process of taking new reactions from conception to fruition, the donor properties and steric profiles of the ancillary ligands, along with reaction conditions, provide the major tools for optimization. Simple metrics for donor and steric properties have proven to be powerful tools for catalyst optimization, especially in late transition metal chemistry. Perhaps one of the most familiar citations in chemistry is by Chadwick Tolman published in *Chemical Reviews* in 1977 on steric and electronic effects in phosphine chemistry.[1] Tolman's cone angle gave a reasonable one-parameter metric for sterics. The energy of the totally symmetric carbonyl vibration in $Ni(CO)_3(PR_3)$ complexes gave a useful single-parameter metric for donor properties.

Using CO stretching frequencies to parametrize later transition metal ligand effects predates this Tolman review, however. For example, Wilkinson and co-workers in 1959 reported the IR stretching frequencies of transition metal carbonyls bearing amine/phosphine donors and reported "the resulting negative charge on the metal atom $R_3N^+-M^-$ may...be dissipated by increasing the bond orders in the M−C−O system".[2] They reported a steady rise in carbonyl stretching frequencies on replacement of phenyl groups in $(Ph_3P)_3Mo(CO)_3$ with chlorine until reaching $(Cl_3P)_3Mo(CO)_3$.[3]

Parameterization methods have been extensively used in a large variety of low-valent and late transition metal catalytic reactions.[4] Similar quantitative measures are a mainstay of physical organic chemistry; for example, the reactivity of

Received: November 22, 2011
Published: December 21, 2011

   dx.doi.org/10.1021/ic202524r | *Inorg. Chem.* 2012, 51, 1187−1200

compounds with pendant aryl groups is often predicted or explained by parameters developed by Hammett, Taft, and others.[5] Quantitative structure−activity relationships (QSAR) have developed into a powerful tool for other areas as well, e.g., pharmaceutical design.[6]

In contrast, methods for determining donor properties of ligands on metal complexes in higher formal oxidation states are less well-known. This is despite the fact that the donor properties of common ligands on earlier, higher-valent metals are likely to be quite different from later, lower valent metals in many cases because of differences in the number and type of empty acceptor orbitals.

If the ligands in question are members of a closely related series, e.g., *para*-substituted phenoxides, one can try to draw analogies to pK_a or Hammett parameters; however, the investigator is left wondering if these are good measures for the transition metal system in question. This problem is only exacerbated if the ligands are more dissimilar, such as comparing phenoxide to iodide to indolyl. Different donor atoms, e.g., oxygen versus nitrogen, or even different hybridization of the same donor atom may affect radial extensions for the orbitals even if the frontier orbitals are of similar shape, which could lead to quite different bonding properties because of the changes in overlap integrals and energies.

While QSAR has been done on early to middle transition metal complexes, these are often studies of specific systems with limited applicability to high valent metals in general. For example, extensive QSAR has also been done in recent computationally driven studies like the one published by Jensen and co-workers on Grubbs's catalyst.[7] Steric and electronic parametrizations have been applied to metallocene[8] and nonmetallocene[9] polymerization catalysts using a variety of techniques varying from simply categorizing ligand types to numerical quantization of ligand properties. In addition, electronic influence of substituents on *ansa*-metallacene complexes has been examined in great detail.[10]

For our investigations in titanium catalysis,[11] we sought a method for the comparison of a large variety of monodentate ligands on early metals to aid in ligand design and for understanding spectroscopic and reactivity trends within various transition metal systems.

In this study, we discuss the use of a large selection of monodentate ligands on the d^0 metal complex, $NCr(NPr^i_2)_2X$, where X is an adjustable monodentate ligand. As will be shown, the synthetic versatility of this framework allows synthesis of a series of compounds for evaluation. In this manuscript, we limit the discussion to monoanionic X;[12] however, these range from common ancillaries used in organometallic chemistry like amido and alkoxide to classical Werner-type ligands such as halides, cyanide, and thiocyanate. The system's design lends itself to a one parameter quantification of donor properties similar to the $Ni(CO)_3L$ system commonly used for late transition metal ligands. Steric metrics for the ligands are provided, and possible steric interference is discussed.

RESULTS AND DISCUSSION

I. System Used for Ligand Parameterization. The method chosen here for the experimental parametrization of ligand donor properties on high valent metal centers involves the use of chromium(VI) nitrido complexes with diisopropylamido ancillaries. All of the compounds in this study are of the type $NCr(NPr^i_2)_2X$, where X is a monoanionic ligand. These complexes are readily prepared, as will be shown in the next Section. In addition, the amido ligands display variable rotation rates dependent upon the donor properties of X. The rotation of the diisopropylamido ligand in these systems has a rate that is readily measured by ^{1}H NMR spectroscopy. In this study, spin saturation transfer was the standard method for ligand rotation rate determination; however, line-shape analysis can also be used and was used for some compounds (vide infra).

Since the compounds are *pseudo*-tetrahedral, the system is not orthoaxial, and the σ- and π-orbitals mix during the bonding interactions with the ligands. This is exemplified in the Angular Overlap Model (AOM) Parameters for a rigorously tetrahedral compound by the energy of the t_2* orbital being parametrized as $e_{t_2}^* = 4/3\ e_\sigma + 8/9\ e_\pi$ where the ligand's σ- and π-donor parameters both contribute to the energy of the triply degenerate orbital. Lowering the symmetry, as is done here, will lead to further mixing, and a single parameter for ligand donor properties is the result.

The highest symmetry available in the nitrido compounds here would be C_{3v} with a formula of $NCrX_3$, where the chromium-nitrido bond is along the *z*-axis. In C_{3v}, the $d_{xy}/d_{x^2-y^2}$-orbitals comprise an e-set, with the p_x/p_y-orbitals having the same symmetry. These e-sets act as both σ- and π-acceptor orbitals for the basal amido ligands. In addition to the π-accepting e-set near the *xy*-plane, there is an e-set composed of the d_{xz}/d_{yz}-orbitals that are involved in strong π-interactions with the nitrido.[13]

In other words, rotation of the amido ligands 90° from where they π-donate into acceptor orbitals near the *xy*-plane to where they could donate into the d_{xz}/d_{yz} orbitals along the nitrido vector causes them to compete with the very strongly donating nitrido. As a result, there is an electronic barrier to rotation around the $Cr-NPr^i_2$ bond determined by the energy difference between the geometries where the amido $CrNR_2$ plane is parallel with the Cr−N(nitrido) vector and where it is perpendicular. Increasing the donor abilities of the ligands in the basal set reduces this difference somewhat, decreasing the barrier for amido rotation through ground-state destabilization.

In short, the stronger a donor X is in a compound like $NCr(NPr^i_2)_2X$, the smaller the barrier to amido rotation is expected to be. Because the σ- and π-systems are strongly mixed, the σ- and π-donor properties of X both contribute to the size of the diisopropylamido rotational barrier. We propose that this isomerization barrier can be used as a measure of the donor ability of X in high valent transition metal systems.

The above arguments can be illustrated using Density Functional Theory (DFT) on the model system $NCr(NH_2)_3$ using B3LYP as the functional. Our initial exploration with this molecule used the 6-31G** basis set, but the calculations were extended to the much larger aug-cc-pVQZ basis set, which provided similar results. Optimization provided a ground state structure where all of the amido ligands are planar and the Cr−NH_2 planes are parallel to the nitrido vector as expected (Figure 1, bottom).

If $NCr(NH_2)_3$ is reoptimized while restricting the dihedral angle in one of the amido ligands to induce rotation, the rotating nitrogen pyramidalizes as the lone pair on the amido approaches the nitrido π-orbitals.[14] In other words, the nitrido prohibits significant π-donation from the rotating amido when it would donate into the same orbital. The energy of the complex increases with increasing amido nitrogen hybridization parameter (λ in sp^λ) from $\lambda = 2$, that is, sp^2, in the ground state to around $\lambda = 2.8$ (Figure 1, plot) at the transition state for the rotation.[15] From the calculations an enthalpic barrier, $\Delta H^\ddagger$, of

dx.doi.org/10.1021/ic202524r | Inorg. Chem. 2012, 51, 1187−1200

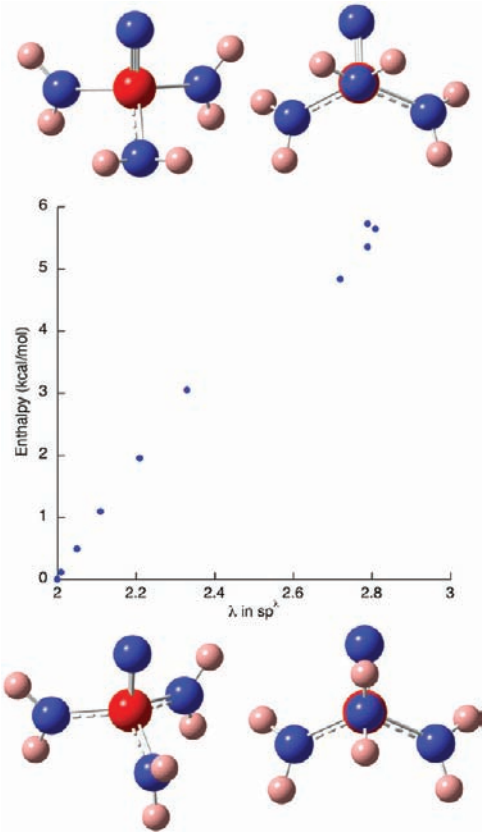

Figure 1. DFT B3LYP/aug-cc-pVQZ computational results for $NCr(NH_2)_3$. On the bottom are two views of the computed ground state, with the right view looking down one of the three equivalent amido-chromium vectors. In the middle is a plot of the hybridization parameter (λ) vs the calculated enthalpic energy of the complex with the ground state set to 0 kcal/mol. On the top are two views of the transition state structure found for rotation of one amido ligand, with the right view looking down the rotated amido-chromium vector.

5.7 kcal/mol was found using the aug-cc-pVQZ basis set. Meanwhile, the Cr−N(nitrido) bond distance seems virtually unaffected by the rotation, varying by less than 0.01 Å over the entire course of the rotation.

The transition state for amido rotation, which had a single negative vibration, was found at 61° in the N(nitrido)-Cr−N(amido)−H dihedral. Figure 1 has images of the ground state and transition state structures. Also in Figure 1 is a plot of λ versus enthalpy. The hybridization parameter increases fairly smoothly up to the transition state, consistent with competition with the nitrido π-donation being the cause of amido pyramidalization.

The amido distance does seem to change slightly with rotation because of bond order effects with the chromium, but the relationship is complicated by electronic adjustments made by the other amido ligands. The average Cr−NH_2 distance in the ground state from the calculations is 1.83 Å. In the transition state, the pyramidalized (rotating) amido distance increases to 1.90 Å, but the amido ligands not undergoing rotation shorten their distance to chromium to 1.81 Å. As a result, the average Cr−NH_2 distance in the transition state is 1.84 Å, essentially identical to the ground state. In other words, rotating one ligand causes ripples of change through the other ligands. It is these indirect changes in the amido ligands because of compensating effects around the metal that we are measuring in this study.

In the actual diisopropylamido complexes used in the experimental studies, this degree of pyramidalization may not be possible for steric reasons. However, the hybridization of the amido nitrogen in the model is illustrative of the type of electronic changes expected on rotation. Donation into the same orbitals as the strongly donating nitrido is energetically unfavorable, and, in the model at least, this competition for the metal's acceptor orbitals manifests as amido rehybridization.

In this study, the $NCr(NPr^i_2)_2$ fragment is held constant, and the barrier to rotation of the diisopropylamido ligands in this constant fragment are what is being measured. The X substituents affect the amido barrier to rotation only indirectly, and the only changes from one complex to another are the electronic and steric components of X in $NCr(NPr^i_2)_2X$.

This system has several advantages for this type of study. First, the compounds prepared thus far have good to excellent thermal stability. Second, the complexes are diamagnetic, allowing easy use of NMR for evaluation. Third, the Cr(VI) nitrido compounds tend to be pseudotetrahedral; we have not observed dimers with bridging X ligands in this system, for example. Fourth, ligands tend to be monodentate on the metal allowing a more uniform comparison between various ligand sets. Even ligands such as carboxylate, with a strong tendency to have higher hapticity in most complexes, only show what appear to be weak secondary interactions with the metal if any (vide infra). Fifth, the $NCr(NPr^i_2)_2X$ complexes are readily prepared from inexpensive reagents with an extraordinary variety of X as will be described next.

II. Preparation of $NCr(X)(NPr^i_2)_2$ Complexes and Characterization. Here, we begin by discussing a new synthetic protocol based on nitrogen-atom transfer for the formation of $NCr(NPr^i_2)_3$ (**1**). All other complexes are prepared by modification of **1**. The synthetic protocols for the production of the other $NCr(X)(NPr^i_2)_2$ complexes will be divided into 7 categories: protonolysis with lutidinium halides, protonolysis with HX, exchange using thallium salts, exchanges between lithium salts and the chromium phenoxide, metathesis using sodium salts, ligand exchange with lithium to zinc transmetalation, and tin(IV)-catalyzed decomposition of a cationic BF_4 salt.

A. Synthesis of $NCr(NPr^i_2)_3$ (1) by Nitrogen Atom Transfer. The starting material for all of this chemistry is the Bradley complex, $Cr(NPr^i_2)_3$, prepared on large scales from $CrCl_3$ and $LiNPr^i_2$ in ethereal solvent.[16] The 3-coordinate compound is soluble in hydrocarbons and crystallizes as large black plates. In the previously reported synthesis of nitrido $NCr(NPr^i_2)_3$ (**1**), black solutions of $Cr(NPr^i_2)_3$ reacted with NO gas to form orange $ONCr(NPr^i_2)_3$, which was deoxygentated with vanadium(III) to form the terminal nitrido.[17]

For this work, a somewhat more straightforward synthesis was used where $Cr(NPr^i_2)_3$ was treated with $NCr(OBu^t)_3$ to give $NCr(NPr^i_2)_3$ (**1**) through a nitrogen-atom transfer (eq 1). Yellow $NCr(OBu^t)_3$ is available from chromyl chloride in a one-pot procedure published by Chiu and co-workers.[18] The nitrido was readily separated from the oily $Cr(OBu^t)_3$[19] byproduct by washing with acetonitrile.

$$Cr(NPr^i_2)_3 + NCr(OBu^t)_3 \xrightarrow[1.5\ h]{pentane} NCr(NPr^i_2)_3 \quad (1)$$
$$-Cr(OBu^t)_3 \qquad \mathbf{1},\ 89\%$$

dx.doi.org/10.1021/ic202524r | Inorg. Chem. 2012, 51, 1187−1200

B. Syntheses Using Protonolysis with Lutidinium Halides. Dark beet-red **1** was converted to orange $NCr(I)(NPr^i_2)_2$ (**2**) with 2,6-lutidinium iodide using the published procedure.[20] Using methods similar to the iodide synthesis, we prepared the chloride (**3**) and bromide (**4**) complexes. The syntheses involved the addition of anhydrous 2,6-lutidenium halide to **1** in chloroform at 60 °C (eq 2).

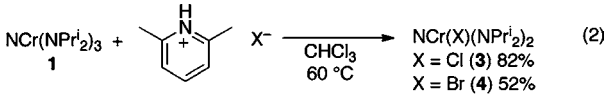

C. Syntheses Using Direct Protonolysis with HX. For this study, a total of 15 complexes were prepared using the direct addition of HX, where X is the new desired ancillary ligand (eq 3). For the synthesis of most alcohols, silanols, carboxylates, and thiolates, direct protonolysis on **1** turned out to be the most convenient and highest yielding methodology. The reactions were carried out using toluene as the solvent for all of these cases, with the exception of triflate where DME/pentane was employed.

The other conditions required for the syntheses varied widely depending on the substrate HX. Some reactions, such as with triflic acid, worked best when started at near frozen temperatures with short stirring times at room temperature. Other substrates were heating for several days to get good conversion; for example, the reaction with 1-adamantanol (HOAd) required heating at 90 °C for 3 days.

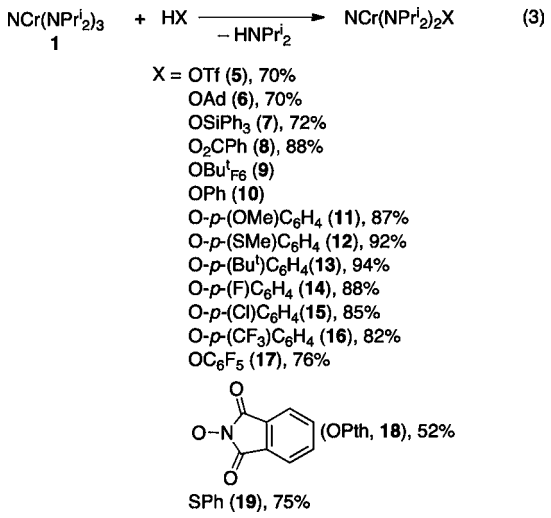

Two of the compounds in eq 3, **9** and **10**, have been previously reported.[21]

D. Syntheses Using Exchange with Thallium Salts. Thallium salts were advantageous in several cases for the production of new $NCr(NPr^i_2)_2X$ complexes. The reactions with iodide (**2**), led to rapid precipitation of TlI, which is readily removed by filtration. The reactions were generally clean, and the use of thallium avoids unwanted reduction processes found using some other reagents (vide infra). Some obvious disadvantages for thallium are the toxicity of the metal and lack of stability with some X substituents. Thallium was employed in the preparation of five of the complexes (eq 4).

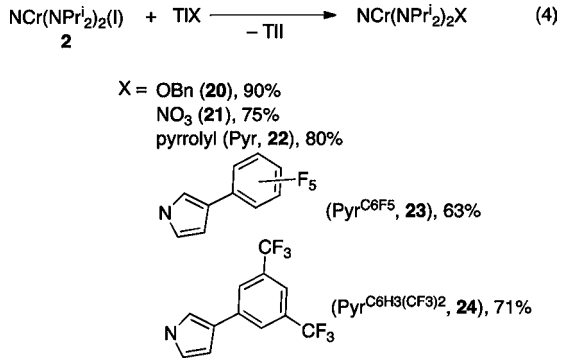

Protonolysis of **1** with HOBn proved to be slow and not very clean. Using TlOBn, $NCr(NPr^i_2)_2(OBn)$ (**19**) was prepared in good yield from iodide **2**. Hexanes or toluene were used for the majority of these transmetalation reactions.

Likewise, commercially available $TlNO_3$ gave $NCr(NPr^i_2)_2(NO_3)$ (**20**); in this case, tetrahydrofuran (THF) was advantageous because of the low solubility of the thallium salt in most other solvents.

Thallium was especially useful for pyrrolyl and pyrrolyl derivatives. The thallium salts were readily available by simple reaction of TlOEt with the *NH*-pyrrole. The thallium pyrrolyls seemed at best sparingly soluble in any solvent with which they did not react, as evinced by being ^{1}H NMR silent as saturated solutions in several solvents, but the compounds reacted readily and cleanly with the iodide **2**. The chromium complexes of pyrrolyl (**22**) and two different 3-aryl-pyrroles (**23** and **24**, eq 4) were prepared using this procedure.

E. Syntheses Using Exchange with Lithium Salts. When using lithium reagents, reduction of iodide **2** to the known μ-nitrido chromium(V) dimer[20] $[NCr(NPr^i_2)_2]_2$ was evident. Transmetalation using the phenoxide **10** was often more successful with these reagents, and this method was used to prepare the indolyl (**25**), carbazolyl (**26**), and *N*-methylanilide (**27**) complexes (eq 5) from their respective lithium salts. A similar method was used in the conversion of $NCr(OPh)_2(NPr^i_2)$ to $NCr(CH_2SiMe_3)_2(NPr^i_2)$ in work from the Cummins laboratory.[21]

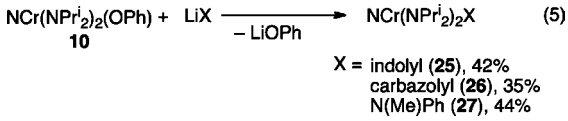

F. Syntheses Using Exchanges with Sodium Salts. The three complexes $NCr(NPr^i_2)_2(X)$, where X = NCO (**28**), NCS (**29**), and CN (**30**), were prepared (eq 6) from the commercially available NaX salts and $NCr(NPr^i_2)_2(I)$ (**2**). The main difficulty with the reactions was the low solubility of these reagents in organic solvents. Acetonitrile was used as the solvent, and reactions required relatively long reaction times and/or mild heating. In the case of NaCN, 1 equiv of 15-crown-5 was advantageous.

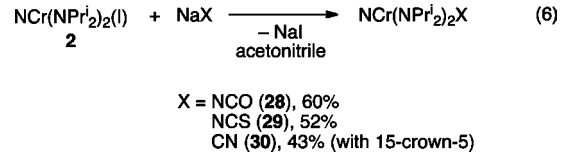

G. Ligand Exchange with Zinc Transmetalation. For probing steric effects in the barriers to rotation (vide infra), it was desirable to synthesize the dimethylamido complex

dx.doi.org/10.1021/ic202524r | Inorg. Chem. 2012, 51, 1187–1200

$NCr(NPr^i_2)_2(NMe_2)$ (**31**) for comparison with $NCr(NPr^i_2)_3$ (**1**). The most fruitful route (eq 7) we discovered to **31** involves treating $ZnCl_2$ with $LiNMe_2$ in DME/THF solvent. Presumably, a $Zn(NMe_2)_2$ solvate or perhaps an amido-containing zincate complex is prepared. This mixture does transmetalation with iodide **2** more cleanly than with the lithium salt alone. Attempts to prepare **31** directly from **2** with $LiNMe_2$ resulted largely in reduction.

$$\underset{\mathbf{2}}{NCr(NPr^i_2)_2(I)} + 8.5\ LiNMe_2/4.25\ ZnCl_2 \xrightarrow[THF/DME]{} \underset{\mathbf{31}\ 70\ \%}{NCr(NPr^i_2)_2(NMe_2)} \quad (7)$$

H. Tin(IV)-Catalyzed Decomposition of a Cationic BF_4 Salt. Many different methods were tried in attempts to prepare the fluoro complex. Success was finally found when we generated a cationic complex by treatment of the iodo **2** with $AgBF_4$ in the presence of DMAP to form $[NCr(NPr^i_2)_2(DMAP)]BF_4$ (**32**).[12] Thermal decomposition of this complex does form small amounts of fluoride $NCr(NPr^i_2)_2(F)$ (**33**) but also gives a large amount of unidentified side-products. In one attempt to form the fluoride by transmetalation, we reacted **32** with $FSnBu^n_3$, which gives fluoro **33** relatively cleanly (Scheme 1).

Scheme 1. Synthesis of $NCr(NPr^i_2)_2(F)$ (33)

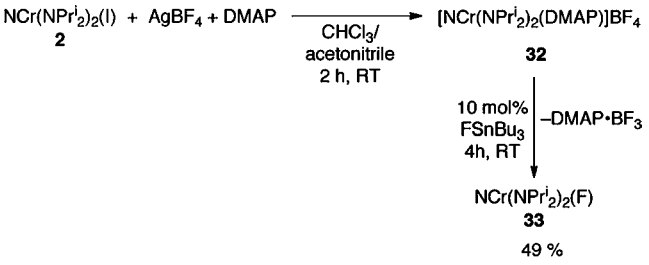

Subsequently, we found that $FSnBu^n_3$ could be used catalytically. It appears that Sn(IV) complexes can catalyze the decomposition of **32**, as can some other mild Lewis acids.[22] The expected byproduct, $DMAP{\cdot}BF_3$, was easily detected in the ^{19}F NMR spectrum of a reaction to form **33** carried out in an NMR tube.[23]

III. Single-Crystal X-ray Diffraction Studies. All of the compounds of the formula $NCr(NPr^i_2)_2(X)$, where X is an anionic substituent, have been structurally characterized.[24] As might be expected, the Cr–N distances, both nitrido and amido, are not exceedingly sensitive to changes in X outside the error limits of the X-ray diffraction experiment. All of the compounds exhibit diisopropylamido ligands with the $Cr–NC_2$ amido planes parallel to the Cr–N(nitrido) vector, as expected from the electronic structure (vide supra). Discussion of the X-ray structure of each compound would be gratuitous; however, a few of the more salient features will be addressed in this section.

The structural characterization on so large a number of derivatives was carried out predominately to facilitate the steric analyses discussed below, to determine if there were any secondary interactions (e.g., bidentate ligands), and to ascertain if any of the structural parameters might reliably correlate with the electronic and steric features. The presentation of the results here will be brief; cif files and crystallographic tables can be found in the Supporting Information.

The donor abilities of the X ligands did not have a large impact on the chromium-nitrido distance. Indeed, the nitrido distance is very similar for all the complexes measured thus far. For example, the nitrido distance in the poorly donating triflate (**5**), strongly donating and relatively small benzyloxy (**19**), and the large and strongly donating diisopropylamido (**1**) were found to be 1.543(3), 1.543(2), and 1.544(3) Å, respectively. The full range of Cr–N(nitrido) values is 1.524(3) in nitrate **21** to 1.553(4) Å in O-*p*-$(CF_3)C_6H_4$ **16**. However, there is no obvious correlation between this distance—or, for that matter, any other metric parameters investigated—and any of the steric or electronic parameters derived.

The two chromium-diisopropylamido bond distances were generally the same within error. The only exception in this list of compounds was for carbazolyl **26**, which had Cr–N(diisopropylamido) distances of 1.796(2) and 1.833(2) Å. The carbazolyl plane is tilted from the Cr–N(nitrido) vector (Figure 2) and, according to the space filling models, there is

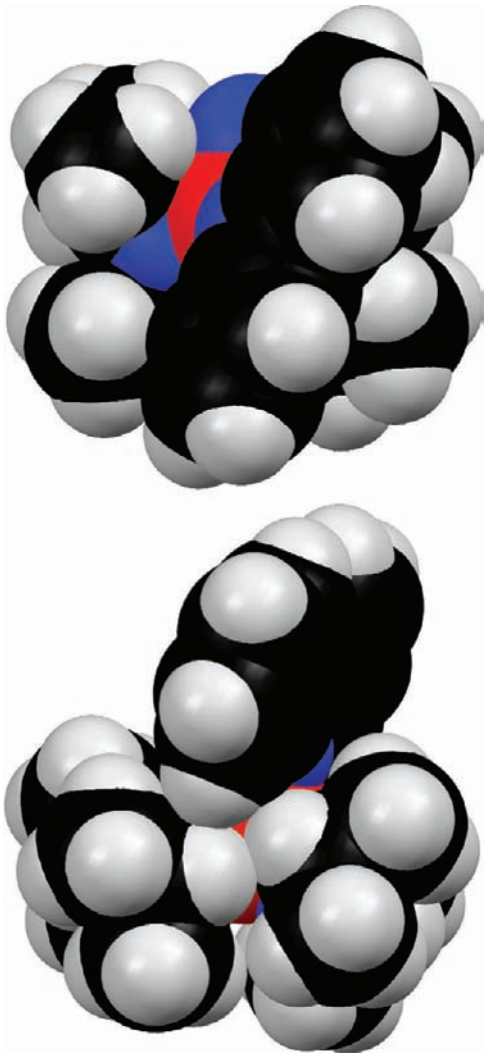

Figure 2. Spacefilling views of $NCr(NPr^i_2)_2$(carbazolyl) (**26**). The top view is looking down the Cr–N(carbazolyl) bond showing the tilting of the heterocyclic framework. The bottom view is *anti* to the nitrido and shows the tilted carbazolyl ring's close contacts with one of the *iso*-propyl groups.

steric clash between the aromatic ring of the carbazolyl *anti* to the nitrido and a diisopropylamido ligand. The longer $Cr–NPr^i_2$ distance is associated with the amido closer to the tilted carbazolyl on the side *anti* to the nitrido (the left NPr^i_2 group in the top of Figure 2). However, the average $Cr–NPr^i_2$ distance

dx.doi.org/10.1021/ic202524r | *Inorg. Chem.* 2012, 51, 1187–1200

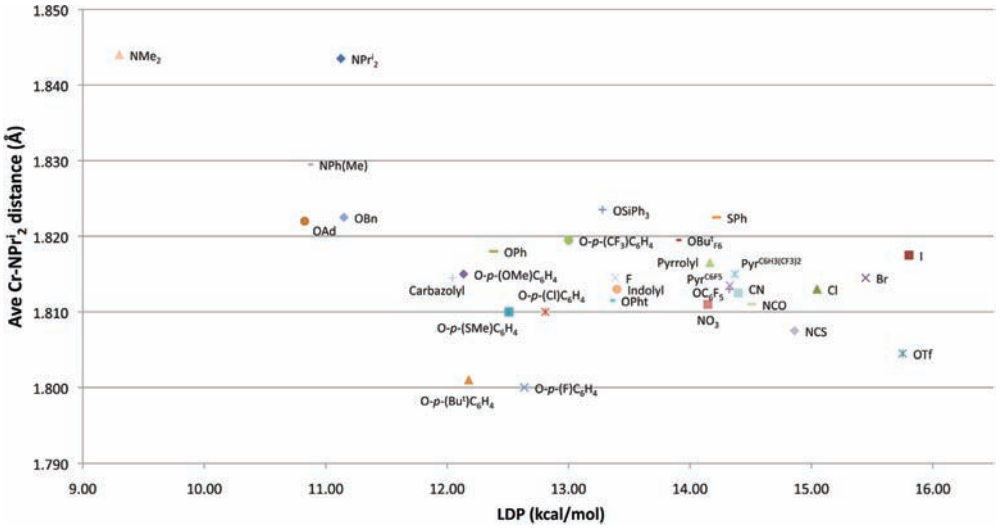

Figure 3. Plot of average Cr−NPr$^i_2$ distance (Å) vs the donor ability of X (LDP in kcal/mol).

in **26** is similar to the other compounds, and it appears that the steric influence of the carbazolyl is mostly to differentiate the two diisopropylamidos in the solid state. (The two diisopropylamido groups are equivalent in solution.)

The NCr(NPr$^i_2$)$_2$ molecular fragment showed some variability in its metric parameters. For example, the amido-chromium-amido angle varied from 116.1(5)° (X = N(Me)Ph **27**) to 124.9(1)° (X = CN **30**), and the average Cr−N(amido) distances varied from 1.805(3) Å (X = OTf **5**) to 1.842(2) Å (X = NPr$^i_2$ **1**). While attempted correlations with these metric parameters and the donor parameters are suggestive, plots of N(amido)−Cr−N(amido) angles and Cr−N(amido) distances with either the steric parameters or the donor properties gleaned from the NMR data showed no strong correlations.

Steric factors seem evident in the tris(diisopropylamido) complex **1** according to other data (vide infra), but it is difficult to discern this from the X-ray diffraction studies alone. The average Cr−N(amido) distance in the published structure for **1** is 1.842(3) Å. This distance in **1** is somewhat larger than many of the derivatives prepared. For example, the average Cr−N(diisopropylamido) distances for a few derivatives are Cl **3** 1.813(2), OBn **20** 1.823(1), OAd **6** 1.822(7), N(Me)Ph **27** 1.830(2), and OTf **5** 1.805(3) Å. However, the average diisopropylamido distance in **1** is very much in line with the sterically less encumbered NMe$_2$ **31** with average Cr−N distances of 1.842(4) Å; incidentally, **31** was one of the compounds examined that displayed full molecule disorder in the X-ray diffraction experiments. The disorder was fully modeled.

A plot (Figure 3) of the average diisopropylamido distance versus the Ligand Donor Parameter (LDP) described below shows no clear correlation. This may be due to the errors in the structural parameters considering the less donating ligands (toward the right in the plot) do, generally speaking, seem to have shorter Cr−N(amido) distances and the more donating ligands seem to have generally longer distances. However, the scatter in the data is far too large to make anything resembling an accurate correlation. In fact, the shortest Cr−N(amido) averages are found for two aryloxide derivatives with moderate LDP values (vide infra) for this series.[25]

Two compounds, benzoate **8** and nitrate **21**, possibly show weak secondary interactions between Cr and the X ligand. For nitrate containing **21**, the Cr−O distance is 1.973(3) Å, and there is a possible weak interaction with a second oxygen of the nitrate nearly *trans* to the nitrido, which is quite long at over 2.7 Å. For benzoate **8**, which has a similar structure near the metal center, the short Cr−O distance is 1.924(1) Å with a possible interaction with the second carboxylate oxygen that is around 3.0 Å away. The contributions from these secondary interactions of X to the measured donor abilities are unlikely to be large at those distances but are not known.

IV. Measurement of Amido Rotational Barriers and the Ligand Donor Parameters (LDP). Most of the NCr(NPr$^i_2$)$_2$(X) complexes employed in this study exhibit two distinct methyne peaks for the diisopropylamido ligands at room temperature assigned as being *syn* and *anti* to the nitrido substituent. The methyne that is *anti* is assigned as being deshielded relative to the *syn* methyne resonance on the basis of 2D NMR experiments on iodo **2** (see the Supporting Information). A few of the compounds where X is a strong donor ligand, for example, dimethylamido and 1-adamantoxide, have the methynes at or near the coalescence point at room temperature. One of the reasons this system was chosen was that the rate of diisopropylamido rotation was easily measured by ^{1}H NMR spectroscopy. Once the rate constants were known, the Eyring equation was used to determine the free energy barriers to rotation, $\Delta G^{\ddagger}_{rot}$, relative to X.

The rate constant for the exchange of the two methynes in the isopropyls, in the majority of cases, was measured using Spin Saturation Transfer (SST) in the ^{1}H NMR.[26] The ideal temperature for the SST experiment was found to be between −56 °C and +27 °C, depending on the rate of rotation for the particular complex being studied. Detailed descriptions of how the SST experiments and error analyses were done can be found in the Supporting Information. In addition, there is a detailed discussion in the Supporting Information of how the T_1 values were found and the types of T_1 values to use.

For one complex, NCr(NPr$^i_2$)$_2$(NMe$_2$) (**31**), because of instrument limitations, we were unable to reach the slow exchange temperature. Line Shape Analysis (LSA) was used to determine the barrier for the isopropyl exchange rather than SST.

dx.doi.org/10.1021/ic202524r | *Inorg. Chem.* 2012, 51, 1187−1200

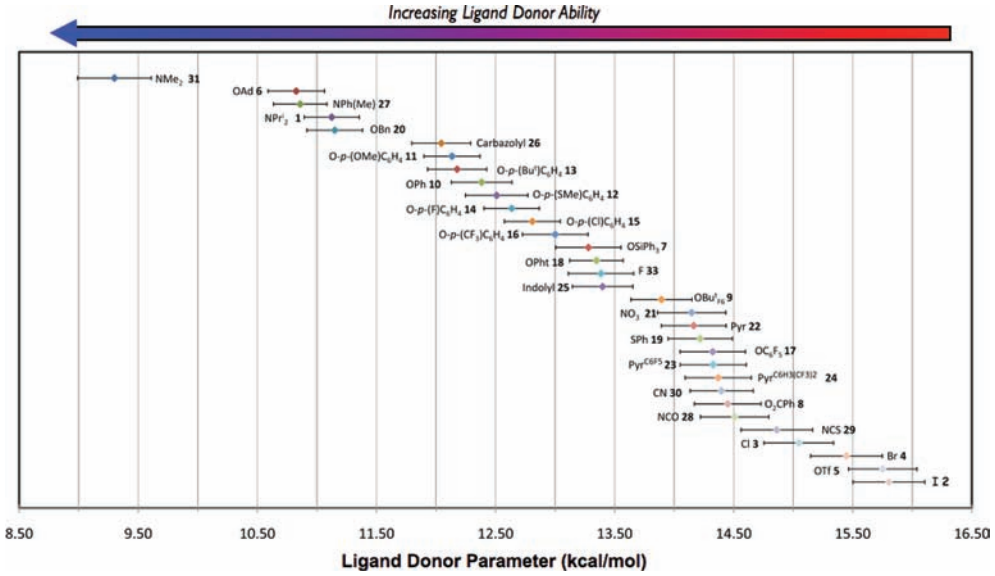

Figure 4. Ligand Donor Parameters (kcal/mol) for various X in $NCr(NPr^i_2)_2X$ with the associated errors.

The X = 1-adamantoxide **6** complex was studied using both LSA and SST for comparison. Both gave the same value to the nearest tenth of a kcal/mol at $\Delta G^{\ddagger}_{rot}$ = 12.8 kcal/mol.

It was expected that the entropy associated with the diisopropylamido rotation would be more or less constant over the series. To investigate this assertion, Eyring plots were done on several of the compounds. The plots were done over as large a temperature range allowable by the kinetics of rotation and our instrumentation. In addition, we explored compounds that varied in $\Delta G^{\ddagger}_{rot}$ and sterics as much as possible. Consequently, the Eyring plots using SST were determined for iodo **2**, benzyloxy **20**, NPr^i_2 **1**, and O-*p*-SMe-C_6H_4 **12**. For these four compounds, $\Delta S^{\ddagger}_{rot}$ was found to be −9, −6, −5, and −3 cal/mol K, respectively. Consequently, the entropy values appear to be small and negative. The entropy values were found from variable temperature (VT) experiments over temperature ranges of 47, 36, 26, and 44 K, respectively. Additional information on the entropy measurements is found in the Supporting Information.

It is most desirable to place the rotational barriers in terms of $\Delta H^{\ddagger}_{rot}$, to remove some of the temperature dependence associated with the measurements. Each compound had to be measured at a temperature best suited for its particular rotation kinetics to measure the rate constant as accurately as possible. Consequently, the SST and LSA data were collected at different temperatures for each complex.

Here, we are always measuring the kinetics for the rotation of a diisopropylamido ligand in a $NCr(NPr^i_2)_2(X)$ complex. *We assume that the* $\Delta S^{\ddagger}_{rot}$ *values for the compounds will all be similar.* Even in cases where the X ligand is quite large and steric effects are likely, that is, for X = NPr^i_2, we have not observed large deviations in $\Delta S^{\ddagger}_{rot}$ values.[27]

The most reliable measurement of entropy, based on where the slow and fast exchange limits occur relative to our available instrumentation, appears to be the value for iodo **2**, which was done over a 47 K interval. As a result, −9 cal/mol K was used as the entropy barrier for most of the compounds.[28] The only compound calculated differently is X = NMe_2 **31**, where the activation barriers were found using a different technique (LSA). The experimental barriers for **31** were determined to be $\Delta S^{\ddagger}_{rot}$ = −4 cal/mol K and $\Delta H^{\ddagger}_{rot}$ = 9.3 kcal/mol.[29]

Under the assumption that entropy differences are minimal, a set of values approximating $\Delta H^{\ddagger}_{rot}$ is obtained. Considering that the values are an approximation based on the assumption of $\Delta S^{\ddagger}_{rot}$ = −9 cal/mol K and their uses for the purposes of this study are more dependent on their relative rather than absolute magnitudes, we call each value a Ligand Donor Parameter (LDP). The LDPs are collected in Figure 4 with horizontal error bars allowing quick distinguishing of ligands that are different outside error limits. The current best numerical parameters are collected in Table 1.

The values in Figure 4 and Table 1 constitute our current best measurements on this particular series for the enthalpies of amido rotation at this time. There are a number of interesting series that one can look at qualitatively. Quantitative comparisons will be discussed in Section VI after discussion of steric influences on rotational barriers.

The halides are in the expected order with iodide being the least donating and fluoride the most donating.

Looking at some monoanionic nitrogen-based heterocycles, it was found that pyrrolyl was a far poorer donor than indolyl, which was a poorer donor than carbazolyl. This is consistent with the expected availability of the nitrogen lone pair for donation in these particular heterocycles. The pyrrolyl ring's aromaticity is dependent upon use of the nitrogen lone pair to reach the 6 π-electrons required by the Hückel rule for aromaticity. As a consequence, the aromatic stabilization energy of pyrrole directly competes with π-donation, which leads to pyrrolyl being a poor π-donor.[30] For indolyl and even more so for carbazolyl, the aromaticity of the 5-membered heterocycles must compete with the 6-membered carbocycle(s) in resonance form contributions to the aromaticity.[31] As a result, the nitrogens in indolyl and carbazolyl seem to donate more strongly to the metal center than pyrrolyl because of the greater availability of their nitrogen-based lone pairs.

The strongest donors explored thus far are dialkylamido and alkoxides, which were thought previously to be strong σ- and π-donors. The weakest donors in the series are those with poor overlap due, in all likelihood, to poor size matches between orbitals such as in iodo and thiophenolate, cf. phenolate, or where the X ligand has a competing π-system that limits π-donation such as NCS, benzoate, and pyrrolyl.

dx.doi.org/10.1021/ic202524r | *Inorg. Chem.* 2012, 51, 1187−1200

Table 1. Values for LDP (kcal/mol) and $\Delta S^{\ddagger}_{rot}$ (cal/mol K) for 1−31 and 33

X =	LDP[a]	$\Delta S^{\ddagger}_{rot}$[e]
NMe_2 (**31**)[29]	9.34 ± 0.32[b]	−4 ± 1[b]
OAd (**6**)	10.83 ± 0.24	
N(Me)Ph (**27**)	10.86 ± 0.23	
NPr^i_2 (**1**)	11.12 ± 0.23[d]	−5 ± 2[c]
OBn (**20**)	11.15 ± 0.23	−6 ± 5[c]
Carbazolyl (**26**)	12.04 ± 0.25	
O-*p*-(OMe)C_6H_4 (**11**)	12.14 ± 0.24	
O-*p*-(Bu^t)C_6H_4 (**13**)	12.18 ± 0.25	
OPh (**10**)	12.38 ± 0.25	
O-*p*-(SMe)C_6H_4 (**12**)	12.51 ± 0.26	−3 ± 4[c]
O-*p*-(F)C_6H_4 (**14**)	12.64 ± 0.23	
O-*p*-(Cl)C_6H_4 (**15**)	12.81 ± 0.23	
O-*p*-(CF_3)C_6H_4 (**16**)	13.00 ± 0.28	
$OSiPh_3$ (**7**)	13.28 ± 0.27	
OPht (**18**)	13.35 ± 0.23	
F (**33**)	13.39 ± 0.27	
Indolyl (**25**)	13.40 ± 0.25	
OBu^t_{F6} (**9**)	13.89 ± 0.26	
NO_3 (**21**)	14.15 ± 0.29	
Pyr (**22**)	14.16 ± 0.28	
SPh (**19**)	14.22 ± 0.27	
OC_6F_5 (**17**)	14.32 ± 0.28	
Pyr^{C6F5} (**23**)	14.33 ± 0.28	
$Pyr^{C6H3(CF3)2}$ (**24**)	14.36 ± 0.28	
CN (**30**)	14.40 ± 0.27	
O_2CPh (**8**)	14.45 ± 0.28	
NCO (**28**)	14.51 ± 0.29	
NCS (**29**)	14.86 ± 0.30	
Cl (**3**)	15.05 ± 0.29	
Br (**4**)	15.45 ± 0.30	
OTf (**5**)	15.75 ± 0.29	
I (**2**)	15.80 ± 0.30	−9 ± 5[c]

[a]Average value from at least 3 measurements for the free energy barrier to rotation. Entropy values were assumed to be −9 cal/mol K except for **31** where the variable temperature LSA value was used. [b]Experimental value from VT LSA. [c]Experimental value from VT SST. [d]Steric effects are quite likely contributing to this LDP. [e]Experimental entropy values in cal/mol K. Errors are from the fits to the Eyring plots.

V. Steric Properties of the Ligands. Coming up with a single parameter for the steric properties of a diverse set of ligands is an inherently inaccurate exercise. One is using a single parameter to describe a 3-dimensional object, which unless that object is a perfect sphere is an incomplete description. However, the Tolman cone angle[1] has been quite successful and gives researchers a parameter for initial optimization of reactions. More recently, Percent Buried Volume ($\%V_{bur}$) calculations have proven useful in determining steric parameters for ancillary ligand sets.[32] Encouragingly, the $\%V_{bur}$ of phosphine ligands agrees nicely with Tolman's cone angles for many standard phosphines. Furthermore, $\%V_{bur}$ are easily calculated from crystallographic data using Cavallo and co-workers web-based utility, Samb*V*ca, and have been used extensively for ligand types like *N*-heterocyclic carbenes.[33]

To determine the $\%V_{bur}$, the ligands are placed in a sphere so that the ligand is the Cr−X bonding distance away from the center. The sphere size is an adjustable parameter meant to approximate the size where ligands affect the primary coordination sphere of the metal. In most instances, a sphere radius of 3.5 Å is used,[34] which is the default in Cavallo's program as well as the distance used by Nolan and co-workers. In Figure 5, there are two examples showing space filling

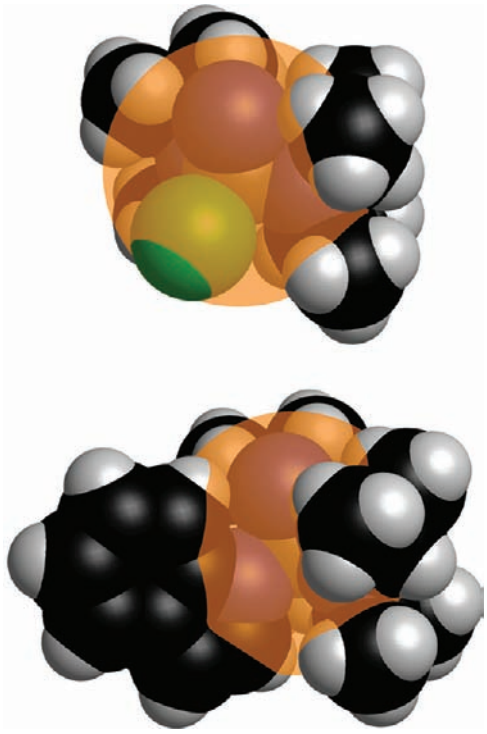

Figure 5. Space filling model of relatively small chloro **3** (top) and large indolyl **25** (bottom). The inscribed orange sphere shows the 3.5 Å radius limit.

models; the orange sphere is 3.5 Å and shows how much of each ligand is included in the calculation. For a discussion and a plot of sphere radius's effect on $\%V_{bur}$ for a selection of ligands, see the Supporting Information. The results of the ligand parametrization using this method are shown in Figure 6.

In addition to $\%V_{bur}$, we also investigated another steric parametrization, the Solid Angle Steric Parameter using the Solid G program.[35] The computational technique works directly from the X-ray diffraction data. The central metal is viewed in some respects as a point source of light, and the ligands block conal access to a sphere around the molecule. An example of the Solid Angle Model is shown in Figure 7 for indolyl **25**, where the molecule is in a similar orientation as in the bottom of Figure 5. The Solid Angle Steric Parameters for the series of X ligands are shown in Figure 8. The *x*-axis values are in percentage of the sphere occupied by the X ligand.[34]

The orderings for many of the ligands change somewhat using the different methods. For example, the Solid G method gives a halide ordering of F > Br > I > Cl because of a mixture of bond distance and radii effects. The halide steric ordering from $\%V_{bur}$ is I > Br > Cl > F and seems to be most greatly affected by atomic radius.[36]

That the complex with X = NPr^i_2 **1** has steric influences on its rotational barrier seems likely. One would expect NPr^i_2 to be a similar or better donor than NMe_2, and yet it has a higher LDP by almost 2 kcal/mol. It appears that sterics are raising the barrier for rotation in this system, and X = NPr^i_2 is the largest ligand investigated by far using both steric metrics.

dx.doi.org/10.1021/ic202524r | *Inorg. Chem.* 2012, 51, 1187−1200

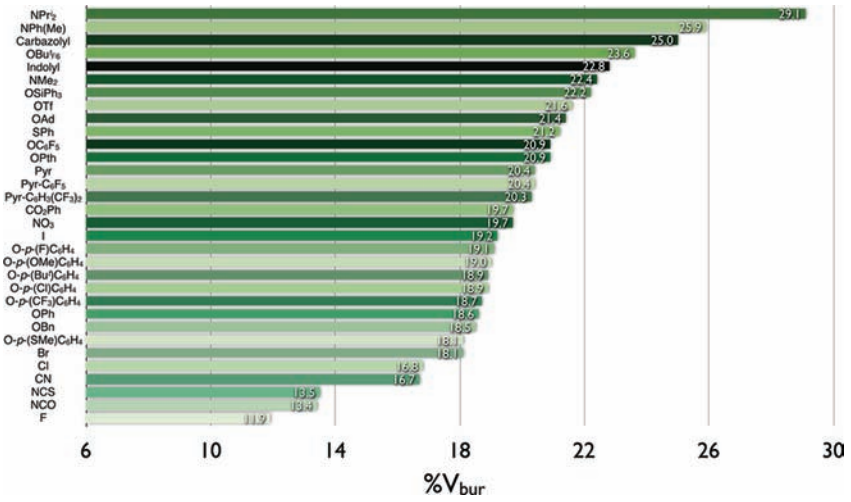

Figure 6. $\%V_{bur}$ for the ligands used in this study. Values are for the percentage volume occupied by the ligand in a sphere of radius 3.5 Å from the chromium center.

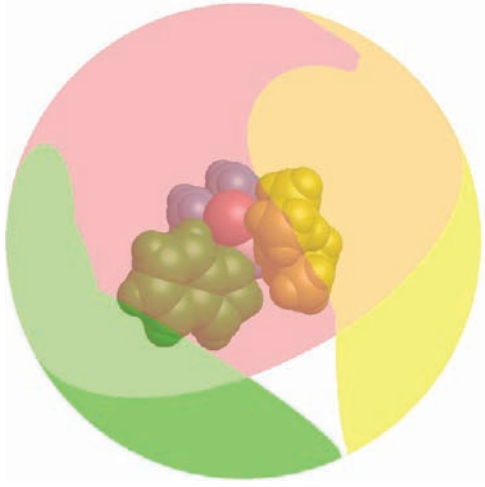

Figure 7. Solid Angle Model from the Solid G program for **25** with indolyl (green), diisopropylamido (yellow and blue), and nitrido (red).

The only compound where steric effects seem certain to be playing a role in the measurement of LDP is NPr^{i}_2 **1**. All other compounds are assumed to have LDPs predominately associated with the electronic barrier to amido rotation as there is currently no compelling evidence to suggest otherwise. Some of the most likely ligands to have unresolved steric effects are $OSiPh_3$, OBu^{t}_{F6}, OAd, N(Me)Ph, indolyl, and carbazolyl, but all of these have steric metrics below NPr^{i}_2. If other ligands do have steric effects on the amido rotational barrier, their observed LDPs are likely upper limits, and they are electronically more donating than observed.

VI. Applications and Comparisons with These New Electronic Parameters. We conclude the Results and Discussion Section by comparing the LDP data quantitatively with different systems from the literature. In these types of applications, the LDP values in Figure 4 and Table 1 are used much as CO stretching frequencies may be used in alternative late transition metal applications, as arbitrary numbers (in the case of LDP inversely) proportional to the donor ability of the ligand of interest.

A. Comparison of LDPs with pK_a Values of the HX Compounds. First, we investigated if the LDPs found in this

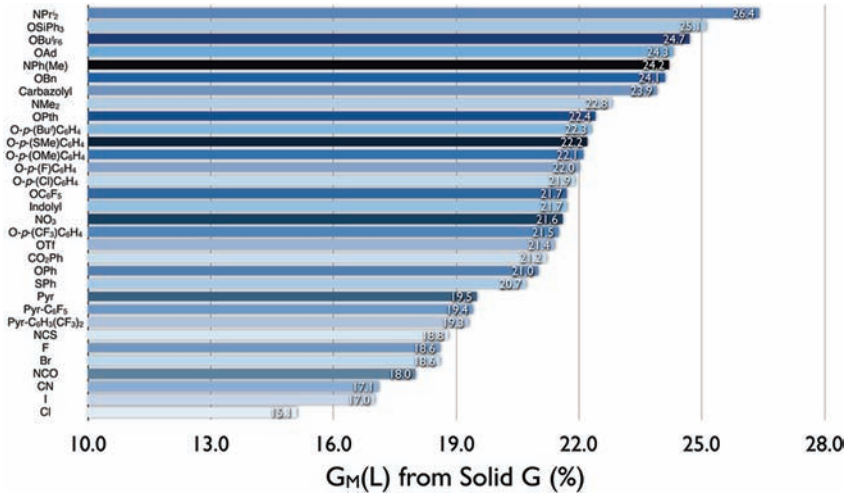

Figure 8. Percentage of the chromium coordination sphere shielded, $G_M(L)$, from the Solid G program for the ligands used in this study.

dx.doi.org/10.1021/ic202524r | Inorg. Chem. 2012, 51, 1187−1200

study correlated to the pK_a of the substituents used. As shown in Figure 9, there is no strong relationship. This is to be

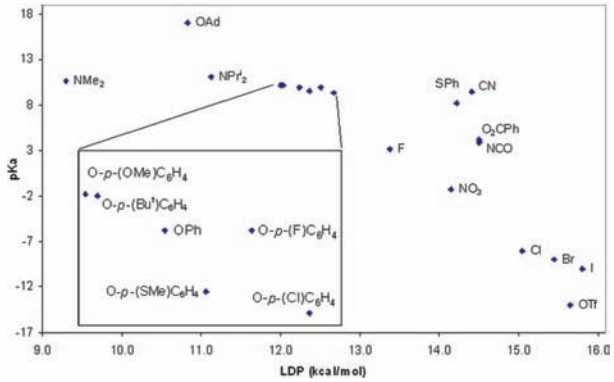

Figure 9. Plot of pK_a in water versus LDP. The inset is an expansion of the region containing the phenoxides.

expected considering the numerous size and orbital makeup differences between the proton and the transition metal system under study.

At best, pK_a can give one a sense of the σ-donor ability of the X ligand when attached to a proton. Perhaps this is the reason for the linear correlation for pK_a and LDP that seems to exist in the plot between the heavier halides I, Br, and Cl where π-effects to the metal are likely minimal. However, pK_a would be expected to give no information on π-donor ability, which is perhaps why fluoride is not on the same line with its heavier congeners.

Other closely related series, such as the phenoxides (inset in Figure 9) may show some trend with pK_a. However, relating ligand acidity to ligand donor ability is likely to be of dubious quality, especially if strong π-effects are present.

B. Phenoxides: An LDP Comparison with Hammett Parameters. Hammett parameters are a reliable and well-worn method for examining electronic effects in a variety of systems with, in large part, *para*-substitution on an arene.[5] To determine if there was a correlation between LDP and Hammett σ_p, we generated the set of *para*-substituted phenoxides **10**–**16**. The full range of LDP differences in the series studied from *para*-OMe to *para*-CF_3 is 12.14 to 13.00 kcal/mol with errors around 0.25 kcal/mol. While values at the extremes of this subset are different outside the errors, many of the values within the series are not distinguishable with these error limits. However, plotting this series of LDP values versus the Hammett Parameters (σ_p) for the substituents shows a good linear correlation considering the error bars on the LDP (Figure 10).

C. Evaluation of ^{13}C NMR Chemical Shifts in Tungsten Metallacycles using LDP. In some cases, spectroscopic data known to change with donor properties of ligands may be correlated with LDP. In 2008, our research group published a study on the reactivity and properties of an unusual class of metallacycles with tungsten–carbon double bond character.[37] Included in this study were NMR spectroscopic data for the series and reactivity in carbonyl olefination reactions for the chloride complex with various additives.

The addition of 2 equiv of cyclooctyne to W(NAr)$_2$Cl$_2$(DME) results in the formation of W(=C_8H_{12}=C_8H_{12}=NAr)(NAr)Cl$_2$ (Figure 11). Substitution of the

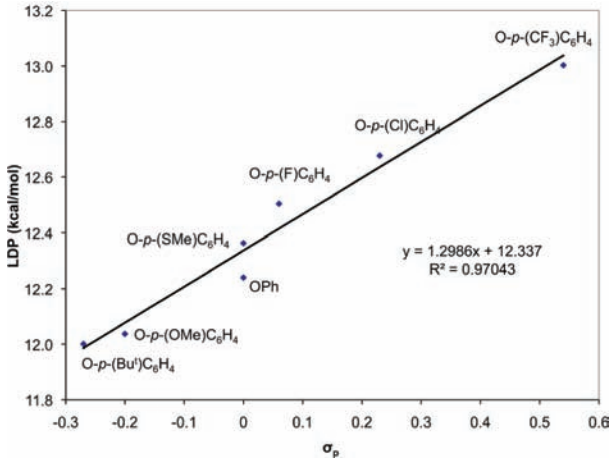

Figure 10. Plot of LDP vs Hammett parameters for the aryloxide complexes.

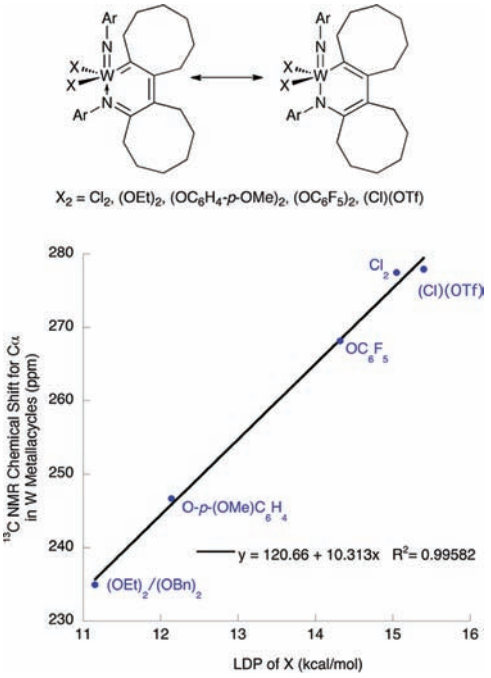

Figure 11. Plot of the ^{13}C NMR chemical shift for the carbon directly bonded to tungsten in W(=C_8H_{12}=C_8H_{12}=NAr)(NAr)X$_2$ versus the donor ability of X found in this work with a linear fit.[37–8].

chlorides for other X ligands leads to structural changes in the complexes and changes in the ^{13}C NMR chemical shift of the carbon bonded to tungsten. These changes may be viewed as being the result of differing contributions between the alkylidene-imine (left) and alkyl-amido (right) resonance forms. In the paper, we simply stated that the values for the chemical shifts changed as "might be expected" with OEt higher than O-*p*-(OMe)C_6H_4 higher than OC_6F_5.[37] Whereas, for chloride and triflate, also included as X ligands in the paper, it was more difficult to discern their donor properties versus these alkoxides.

Using the LDP and plotting versus the ^{13}C chemical shifts, one sees a good correlation between the ligand donor ability as measured in this work across the available ligand sets in the tungsten system and the NMR data reported (Figure 11).[38] The chemical shifts of the α-carbons in the metallacycles do

dx.doi.org/10.1021/ic202524r | *Inorg. Chem.* 2012, 51, 1187–1200

indeed correlate with the donor abilities of the X ligands across the entire range of compounds produced in the tungsten study. The linear relationship between LDP and the ^{13}C NMR chemical shift is exceptionally good (R^2 = 0.996).

D. Comparison Between the AOM of Cr(III) Complexes and the SST Determined Donor Values. In this study, we were able to include several classic Werner-type ligands and determine their donor properties in this Cr(VI) system. In these traditional coordination compounds, the donor properties are usually determined using visible absorption data in conjunction with Ligand Field Theory. The values can also be parametrized using the Angular Overlap Model as σ- and π-donor energies, e_σ and e_π respectively,[39] of individual X.

In Figure 12 is a plot of $e_\sigma + e_\pi$ for chromium(III) complexes from the experimentally determined AOM values[40] versus the

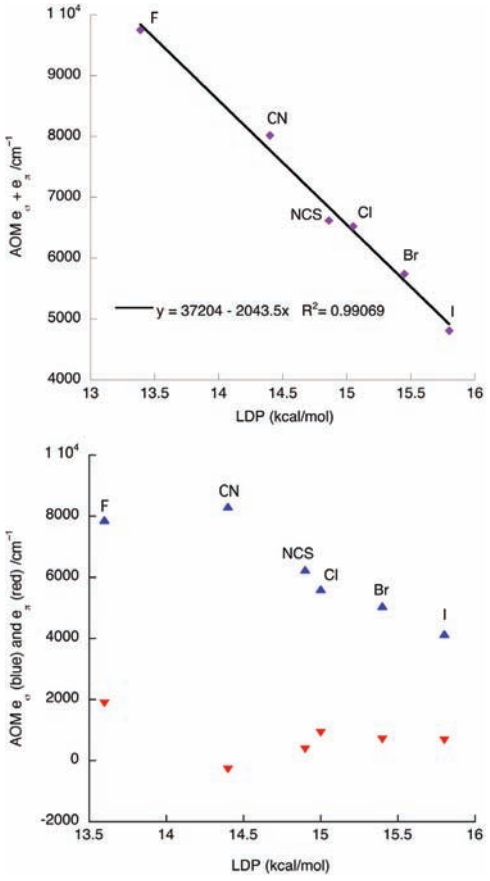

Figure 12. Plot of $e_\sigma + e_\pi$ for chromium(III) complexes from experimentally determined AOM values versus the LDP for X (top). Plot of e_σ (blue) and e_π (red) parameters versus the LDP for X (bottom).

donor ability of X found in this study, which shows a good linear correlation between the two parametrization systems. Also in Figure 12 is a plot of the individual $e_\sigma + e_\pi$ parameters versus LDP (bottom). The correlation with either the e_σ or the e_π parameter alone is not nearly as good as their sum.

E. Comparison Values from Electronic Spectra of Cp$_2$TiX Complexes.* In 1996, Lukens, Smith, and Andersen[41] reported a "π-donor spectrochemical series for X" in Cp*$_2$TiX titanium(III) compounds with a large number of X ligands. The study employed electron paramagnetic resonance (EPR) and absorption spectroscopy to elucidate the electronic structure of d^1 titanium complexes. Of specific interest in the context of this paper, Andersen and co-workers report the singly occupied a_1 to b_2 energy gap, which "depends directly upon the π-donor ability of X". Mach and co-workers have since extended the system to include additional alkoxide ligands.[42]

A plot of the energy gap between a_1 (approximately nonbonding)[43] and the b_2 π-antibonding orbital (ΔE_{xz}) in Cp*$_2$TiX Andersen complexes versus LDP for all X in common between the two studies is shown in Figure 13 (blue and red

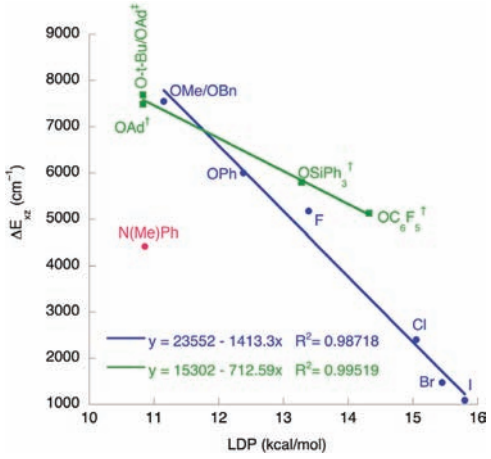

Figure 13. Plot of ΔE_{xz} in wavenumbers (cm^{-1}) [Andersen data[41] (red and blue circles), Mach's data[42] (green squares)] versus LDP (kcal/mol) for X. For the data represented by circles, methylcyclohexane was the solvent. The data represented by green squares were taken in either hexane (‡) or toluene (†).[44].

circles). In the case of X = OMe, the value for ΔE_{xz} was correlated with the LDP value for OBn in the plot (blue line). The obvious outlier is X = N(Me)Ph (red circle), which is well away from what seems to be a linear correlation between the Cp*$_2$TiX spectroscopic data and LDP. Andersen and co-workers centered much of their discussion on the differences between X = N(Me)Ph and the other compounds, and this is quite obvious in Figure 13 as well. Also plotted in Figure 13 are Mach's data (green squares) on Cp*$_2$TiX, where we used our X = OAd data for their X = OBu^t example.

There are several indications that the X = N(Me)Ph in Cp*$_2$TiX has little or no π-effects to the nitrogen; although there are indications of agostic effects to the methyl.[41] In the structure from X-ray diffraction, the Cp*(centroid)−Ti−N−Me average dihedral in the X = N(Me)Ph complex is 86.9°. In other words, the large N(Me)Ph ligand rests in the plane bisecting the Cp*−Ti−Cp* unit, and the nitrogen lone pair is orthogonal to the empty orbital of appropriate symmetry to act as an acceptor. Consequently, the experimental Ti−N bond distance is quite long at 2.054(2) Å. This is similar to Ti−N(pyrrolyl) distances,[30] usually a much weaker donor than N(Me)Ph (vide supra). This distance is also much closer to the Ti−N single bond distance of 2.07 Å than the Ti═N distance of 1.77 Å using Pyykkö's radii.[45] In contrast, Ti−NMe$_2$ distances, where there is a strong dative π-bond, are typically ~1.90 Å.[46]

It can be concluded that the lack of correlation for X = N(Me)Ph is due to a deficiency of π-bonding in the Cp*$_2$TiX system because of steric effects that do not allow the amido to reach the electronically preferred geometry, a fact readily seen

dx.doi.org/10.1021/ic202524r | Inorg. Chem. 2012, 51, 1187−1200

in both the X-ray diffraction study and in correlations with LDP.

If one examines the X = N(H)Me complex of Cp^*_2TiX, the amide is rotated much closer to where maximal overlap with the π-acceptor orbital (b_2) would be possible. The Cp*-(centroid)−Ti−N−Me dihedral for this compound is 13.2°. However, the Ti−N bond, 1.955(5) Å, is slightly longer than the average Ti−NMe_2 bond in the CSD database.[46] This lengthened bond may be due to steric clash with the Cp* ligands.[47]

Overall, the LDPs correlate fairly well with the Cp^*_2TiX spectroscopic data in cases where steric effects are not apparent, that is, all X ligands in common between the two studies except for where the X ligand is an amido derivative.

CONCLUDING REMARKS

Changing metals, changing formal oxidation state, and other ligands on the metal can greatly alter donor properties of ligands. These types of single parameter studies should not replace full mechanistic and computational studies for systems; instead, this is a quick technique that will hopefully be useful in the discussion of properties and mechanisms for metal complexes at low d-electron counts. If a series of ligands for a particular system correlate well to LDP and one does not, it might indicate steric influences, hapticity differences between the chromium system here and the system under study, or other effects are important for that particular compound (for an example see X = N(Me)Ph in Section VI E above). If the system under study does not correlate at all with LDP, there are any number of possible explanations ranging from differences in ligand donor properties, differences in metal acceptor properties, steric interactions, or simply a lack of correlation of the property being measured with ligand donor ability.

In the last segment of the Results and Discussion Section, we attempted to correlate these new LDP values with data from the literature. In the cases discussed above, the values that do correlate, i.e., those other than pK_a, did so linearly. It should be kept in mind, however, that there is no reason to assume that all correlations between LDP parameters and data determined using numerous techniques on various systems will always be linear. In addition, more involved methods than the single parameter %V_{bur} and Solid Angle methods may be required for accurate comparisons of sterics in some systems as well.

The absolute values above consititute our current best evaluations of these ligands. Improved techniques and instrumentation for the determination of ligand donor abilities in this system may lead to improved values in the future.

There are obvious ligand types that would be useful to include in a series of this type that have not yet been prepared for parametrization of their donor properties. We are continuing to expand the series presented here. Current plans include the characterization of cationic chromium(VI) nitrido systems with neutral X ligands and a selection of organometallic ligands, which are being prepared for evaluation.

Parameterizations of this type have seen some historical success in explaining reaction mechanisms and trends in reactivity. For example, Basolo, Pearson, Burdett, and many others have used the Angular Overlap Model extensively in this regard especially for later transition metal systems.[48] It is hoped that this method of ligand parametrization will be useful in catalysis studies ongoing in our group and others on high valent metal complexes.

ASSOCIATED CONTENT

Supporting Information

Experimental details and characterization for the production of all the compounds used in the study. ^1H and ^{13}C NMR spectra for all new compounds. Data for the X-ray diffraction experiments in the form of a cif file. Plot of radius versus % V_{bur} for several ligands. Details on the spin saturation transfer experiments. Details on propagation of error to find LDP values. 2D NMR on **2** and assignments. Details on %V_{bur} and Solid G calcs. This material is available free of charge via the Internet at http://pubs.acs.org.

AUTHOR INFORMATION

Corresponding Author

*E-mail: odom@chemistry.msu.edu.

ACKNOWLEDGMENTS

The authors, and N.A.M. in particular, express gratitude for the assistance of Dan Holmes and Kermit Johnson with the SST and LSA experiments. Dan Mindiola is thanked for his role in the development for the new synthesis of **1**. We also thank Ilia Guzei for aid in the calculation of Solid G parameters. Mitch Smith is thanked for helpful discussion. The financial support of the National Science Foundation CHE-1012537 for this work is greatly appreciated.

REFERENCES

(1) Tolman, C. A. *Chem. Rev.* **1977**, *77*, 313.

(2) Abel, E. W.; Bennett, M. A.; Wilkinson, G. *J. Chem. Soc.* **1959**, 2323.

(3) For other seminal work on CO stretches being used for electronic evaluation see: (a) Nyholm, R. S.; Short, L. N. *J. Chem. Soc.* **1953**, 2670. (b) Cotton, F. A. *Inorg. Chem.* **1964**, *3*, 702. (c) Abel, E. W.; Stone, F. G. A. *Q. Rev. Chem. Soc.* **1969**, *23*, 325. (d) Poilblanc, R.; Bigorgne, M. *Bull. Soc. Chim. Fr.* **1962**, 1301. (e) Strohmeier, W.; Muller, F. J. *Chem. Ber.* **1967**, *100*, 2812. For a recent paper showing effects other than metal electron density can effect these CO stretching frequencies see: (f) Valyaev, D. A.; Brousses, R.; Lugan, N.; Fernandez, I.; Sierra, M. A. *Chem.—Eur. J.* **2011**, *17*, 6602.

(4) For a few representative examples see: (a) Maldonado, A. G.; Hageman, J. A.; Mastroianni, S.; Rothenberg, G. *Adv. Synth. Catal.* **2009**, *351*, 387. (b) Hageman, J. A.; Westerhuis, J. A.; Frühauf, H.-W.; Rothenberg, G. *Adv. Synth. Catal.* **2006**, *348*, 361. (c) Burello, E.; Rothenberg, G. *Int. J. Mol. Sci.* **2006**, *7*, 375. (d) Maldonado, A. G.; Rothenberg, G. *Chem. Soc. Rev.* **2010**, *39*, 1891. (e) Mikhel, I. S.; Garland, M.; Hopewell, J.; Mastroianni, S.; McMullin, C. L.; Orpen, A. G.; Pringle, P. G. *Organometallics* **2011**, *30*, 974. (f) Birkholz, M.-N.; Freixa, Z.; van Leeuwen, P. W. N. M. *Chem. Soc. Rev.* **2009**, *38*, 1099. (g) Gillespie, J. A.; Dodds, D. L.; Kamer, P. C. J. *Dalton Trans.* **2010**, *39*, 2751. (h) Fey, N. *Dalton Trans.* **2010**, *39*, 296. (i) Dröge, T.; Glorius, F. *Angew. Chem., Int. Ed.* **2010**, *49*, 6940.

(5) For a review see: Hansch, C.; Leo, A.; Taft, R. W. *Chem. Rev.* **1991**, *91*, 165.

(6) For some selected recent reviews see: (a) Sprous, D. G.; Palmer, R. K.; Swanson, J. T.; Lawless, M. *Curr. Top. Med. Chem.* **2010**, *10*, 619. (b) Verma, R. P.; Hansch, C. *Chem. Rev.* **2009**, *109*, 213. (c) Michaelidou, A. S.; Hadjipavou-Litina, D. *Chem. Rev.* **2005**, *105*, 3235. (d) Lipinski, C. A.; Lombardo, F.; Dominy, B. W.; Feeney, P. J. *Adv. Drug Delivery Rev.* **2001**, *46*, 3.

(7) Occhipini, G.; Bjørsvik, H.-R.; Jensen, V. R. *J. Am. Chem. Soc.* **2006**, *128*, 6952.

(8) For a few examples see: (a) Möhring, P. C.; Coville, N. J. *Coord. Chem. Rev.* **2006**, *250*, 18. (b) Silveira, F.; de Sá, D. S.; da Rocha, Z. N.; Alves, M. C. M.; dos Santos, J. H. Z. *X-Ray Spectrom.* **2008**, *37*, 615. (c) Kozimor, S. A.; Yang, P.; Batista, E. R.; Boland, K. S.; Burns, C. J.; Christensen, C. N.; Clark, D. L.; Conradson, S. D.; Hay, P. J.; Lezama,

J. S.; Martin, R. L.; Schwarz, D. E.; Wilkerson, M. P.; Wolfsberg, L. E. *Inorg. Chem.* **2008**, *47*, 5365.
(9) Redshaw, C. *Dalton Trans.* **2010**, *39*, 5595.
(10) Zachmanoglou, C. E.; Docrat, A.; Bridgewater, B. M.; Parkin, G.; Brandow, C. G.; Bercaw, J. E.; Jardine, C. N.; Lyall, M.; Green, J. C.; Keister, J. B. *J. Am. Chem. Soc.* **2002**, *124*, 9525.
(11) (a) Swartz, D. L.; Staples, R. J.; Odom, A. L. *Dalton Trans.* **2011**, *40*, 7762. (b) Swartz, L. D.; Odom, A. L. *Organometallics* **2006**, *25*, 6125.
(12) Some cationic complexes using this framework with neutral ligands in place of X have already been prepared, and many others are being developed. It is hoped that this series will allow more overlap with the Tolman ligand maps, which involve mostly neutral ligands. One such complex, **32**, is used as an intermediate to the fluoride reported here. Unpublished results, DiFranco, S.; Maciulis, N.; Odom, A. L.
(13) The orbital labels are an approximation. In actuality, because the $d_{xy}/d_{x^2-y^2}$ and d_{xz}/d_{yz} e-sets have the same symmetry, they will mix as well.
(14) In the calculations, two minima can sometimes be found in the model: one where the lone pair is *syn* to the nitrido and one where it is *anti*. The *anti* isomer is typically the global minimum, which is what is used here.
(15) The hybridization at nitrogen was calculated by taking the calculated angles around the nitrogen and dividing by 3 to get an average hybridization for all the bonds. From the average angle, Coulson's equation for the Directionality Theorem, $\cos \omega_{ij} = -1/((\lambda_i\lambda_i)^{1/2})$, can be used to get the hybridization parameter. In this case where we are simply looking at the average angle, effectively average orbital hybridization, the equation can be simplified to $\lambda = -1/(\cos \omega)$ for looking at equivalent hybrids. (a) McWeeny, R. *Coulson's Valence*; Oxford University Press: Oxford, U.K., 1979. (b) Weinhold, F.; Landis, C. R. *Valency and Bonding*; Cambridge University Press: Cambridge, U.K., 2005.
(16) (a) Bradley, D. C.; Hursthouse, M. B.; Newing, C. W.; Welch, A. J. *Chem. Commun.* **1971**, 411. (b) Bradley, D. C.; Copperthwaite, R. G. *Inorg. Synth.* **1978**, *18*, 112. (c) Bradley, D. C.; Newing, C. W. *Chem. Commun.* **1970**, 219.
(17) (a) Odom, A. L.; Cummins, C. C.; Protasiewicz, J. D. *J. Am. Chem. Soc.* **1995**, *117*, 6613. For related nitrosyl deoxygenation studies see: (b) Veige, A. S.; Slaughter, L. M.; Lobkovsky, E. B.; Matsunaga, N.; Decker, S. A.; Cundari, T. R.; Wolcanski, P. T. *Inorg. Chem.* **2003**, *42*, 6204.
(18) Chiu, H.-T.; Chen, Y.-P.; Chuang, S.-H.; Jen, J.-S.; Lee, G.-H.; Peng, S.-M. *Chem. Commun.* **1996**, 139.
(19) The byproduct $Cr(OBu^t)_3$ is believe to be a soluble dimer. Bradley, D. C.; Mehrotra, R.; Rothwell, I.; Singh, A. *Alkoxo and Aryloxo Derivatives of Metals*; Academic Press: San Diego, CA, 2001.
(20) Odom, A. L.; Cummins, C. C. *Organometallics* **1996**, *15*, 898.
(21) Odom, A. L.; Cummins, C. C. *Polyhedron* **1998**, *17*, 675.
(22) For a similar decompositionof a DMAP containing BF_4 salt see: Huynh, K.; Rivard, E.; Lough, A. J.; Manners, I. *Chem.—Eur. J.* **2007**, *13*, 3431. In addition, the tetraalkyltin $SnBu^n_3$(allyl), which we had on hand, was an active catalyst.It is likely that Sn(IV) is acting as a mild Lewis acid in the reaction,and other acids may catalyzed the decomposition of **32**.
(23) The chemical shift in the ^{19}F NMR of the byproduct in the reaction to produce **33** was identical to the product of the reaction between 1 equiv each of $BF_3{\bullet}OEt_2$ and DMAP in the same solvent.
(24) In this work, 31 of the compounds have been structurally characterized; this number includes the previously reported structures for $NCr(NPr^i_2)_3$ (**1**) and $NCr(NPr^i_2)_2(I)$ (**2**). The only compound not structurally characterized is compound **32**, which was only used as an intermediate in production of the fluoride **33**.
(25) For related studies on aryloxides where no correlation was found between M−O−Ar angle and M−O bond distance see: (a) Steffey, B. D.; Fanwick, P. E.; Rothwell, I. P. *Polyhedron* **1990**, *9*, 963−968. (b) Howard, W. A.; Trnka, T. M.; Parkin, G. *Inorg. Chem.* **1995**, *34*, 5900. (c) Wolczanski, P. T. *Polyhedron* **1995**, *14*, 3335. For systems where alkoxide bond angle does seem to correlate with bond distance see: (d) Tomaszewski, R.; Arif, A. M.; Ernst, R. D. *J. Chem. Soc., Dalton Trans.* **1999**, 1883−1890. (e) Huffman, J. C.; Moloy, K. G.; Marsella, J. A.; Caulton, K. G. *J. Am. Chem. Soc.* **1980**, *102*, 3009.
(26) (a) Jarek, R. L.; Flesher, R. J.; Shin, S. K. *J. Chem. Educ.* **1997**, *74*, 978. (b) Perrin, C. L.; Thoburn, J. D.; Kresge, A. J. *J. Am. Chem. Soc.* **1992**, *114*, 8800. (c) Dahlquist, F. W.; Longmuir, K. J.; Du Vernet, R. B. *J. Magn. Reson.* **1975**, *17*, 406.
(27) We measured the variable temperature SST data for X = Pr^i in two different solvents. In toluene, the activation parameters for rotation were found to be $\Delta H^{\ddagger}$ = 12.4 kcal/mol and $\Delta S^{\ddagger}$ = −2 cal/mol K over a temperature range of 30 °C. In $CDCl_3$, the usual solvent employed for the studies in this paper, the activation parameters for rotation were found to be $\Delta H^{\ddagger}$ = 11.6 kcal/mol and $\Delta S^{\ddagger}$ = −5 cal/mol K over a temperature range of 26 °C. The value of $\Delta H^{\ddagger} = 11.12 \pm 0.23$ kcal/mol in Table 1 is from multiple measurements, consistent with the majority of data in that table.
(28) The amido entropic barriers found here are quite similar to values in the literature for organic amides of various types. For example, the amide rotational barrier in nicotinamide was measured using several different techniques and values from −3 to −10 cal/mol K were obtained. Olsen, R. A.; Liu, L.; Ghaderi, N.; Johns, A.; Hatcher, M. E.; Mueller, L. J. *J. Am. Chem. Soc.* **2003**, *125*, 10125. For some other examples see: Drakenberg, T.; Dahlqvist, K.-I.; Forsén, S. *J. Phys. Chem.* **1972**, *76*, 2178.
(29) Because the value for the NMe_2 derivative was found using a different technique from all the other values, we view its absolute value relative to all the other LDP numbers with some suspicion. However, we have little doubt in its placement as the most donating ligand investigated in this study.
(30) This can be seen inthe metal-nitrogen bond distances of pyrrole versus dialkylamidos.See: Harris, S. A.; Ciszewski, J. T.; Odom, A. L. *Inorg. Chem.* **2001**, *40*, 1987, and references therein for examples..
(31) For a mixed experimental theoretical treatment of aromaticity in indoles and pyrroles see: (a) Hou, D.-R.; Wang, M.-S.; Chung, M.-W.; Hsieh, Y.-D.; Tsai, H.-H. G. *J. Org. Chem.* **2007**, *72*, 9231. For a review on aromaticity of heterocycles see: (b) Balaban, A. T.; Oniciu, D. C.; Katritzky, A. R. *Chem. Rev.* **2004**, *104*, 2777.
(32) For a reviewconcerningthe application of $\%V_{bur}$ see: Clavier, H.; Nolan, S. P. *Chem. Commun.* **2010**, *46*, 841.
(33) (a) Hillier, A. C.; Sommer, W. J.; Yong, B. S.; Petersen, J. L.; Cavallo, L.; Nolan, S. P. *Organometallics* **2003**, *22*, 4322. (b) Poater, A.; Cosenza, B.; Correa, A.; Giudice, S.; Ragone, F.; Scarano, V.; Cavallo, L. *Eur. J. Inorg. Chem.* **2009**, 1759. (c) http://www.molnac.unisa.it/OMtools/sambvca.php
(34) It is certainly possible that no single parameter steric scheme will accurately encompass the influences of a diverse set of ligands like the one found here even if the methodologies are applicable to a relatively narrow group like phosphines and *N*-heterocyclic carbenes. Included in the Supporting Information is a plot of sphere radius versus $\%V_{bur}$ for some ligands. As might be expected, the ligands show different maxima and some of the lines do cross, suggesting the ideal radius is likely system and application dependent. The values here are intended to give a rough measure of sterics for the various ligands.
(35) Guzei, I. A.; Wendt, M. *Dalton Trans.* **2006**, 3991.
(36) The online program for $\%V_{bur}$, Samb*V*ca, does not include all of the halides, and some of these were calculated using an overlapping spheres methods at the appropriate distances. See Supporting Information for details.
(37) (a) Lokare, K. S.; Odom, A. L. *Inorg. Chem.* **2008**, *47*, 11191. See also (b) Lokare, K. S.; Ciszewski, J. T.; Odom., A. L. *Organometallics* **2004**, *23*, 5386.
(38) The value used in the plot for the mixed X ligand set (Cl)(OTf) is the average of the two SST values for the two different ligands. The SST value for OBn was used as the parameter for the ethoxide ligand.
(39) A note of caution for the use of AOM values: the e_π values are often found using the assumption that e_π for NH_3 is equal to zero because of overparameterization within the AOM model. The validity of this assumption has been called into question for some coordination

complexes, most notably Pt(II) where the e_π value for NMe_3 was determined to be well above zero. It is not believed that NH_3 actually does have π-effects; instead, this is attributable to the e_π parameter not being truly zero within the model. For further discussion see ref 39 and (a) Chang, T.-H.; Zink, J. I. *J. Am. Chem. Soc.* **1987**, *109*, 692. (b) Bridgeman, A. J.; Gerlock, M. *Prog. Inorg. Chem.* **1997**, *45*, 179. (c) Schaffer, C. E.; Anthon, C.; Bendix, J. *Coord. Chem. Rev.* **2009**, *253*, 575.

(40) AOM values were takenfrom Hoggard, P. E. *Struct. Bonding (Berlin)* **2004**, *106*, 37, whichwere calculated from splittings in spin-allowed transitions of thecorresponding Cr(III) ammine complexes.

(41) Lukens, W. W. Jr.; Smith, M. R.; Andersen, R. A. *J. Am. Chem. Soc.* **1996**, *118*, 1719.

(42) (a) Gyepes, R.; Varga, V.; Horacek, M.; Kubista, J.; Pinkas, J.; Mach, K. *Organometallics* **2010**, *29*, 3780. (b) Varga, V.; Cisarova, I.; Gyepes, R.; Horacek, M.; Kubista, J.; Mach, K. *Organometallics* **2009**, *28*, 1748.

(43) That the quantitymeasured is exclusively determined by the π-donor ability ofX is of course an approximation. The a_1 orbital is weaklyσ-bonding but largely nonbonding. The b_2 orbitalis orthogonal and its energy is largely determined by the π-bondingof X. For a discussion of the bonding see: Lauher, J. W.; Hoffmann, R. *J. Am. Chem. Soc.* **1976**, *98*, 1729.

(44) The data for X = N(Me)Ph was not used in determining the linear fit to the Andersen data (blue line) shown in Figure 10. The exact cause for the two different slopes of the Andersen and Mach data fits is unknown; however, there are several small differences in the data sets like different solvents, slightly different instrumentation, and possible differences in concentration. In addition, the Andersen data are relative to Cp^*_2TiH as $\Delta E_{xz} = 0$, and we did not adjust the baseline in the Mach data similarly. If the data from the two groups are taken all together and linearly fit, the line obtained is $y = 20761 - 1205x$ with a much worse R^2 of 0.93 versus the $R^2 = \sim 0.99$ obtained fitting the data from the two groups independently. This fit for Mach's data is for only four points from the four new alkoxides in common between our study and Mach's reports. In addition, one of the four points was done with a substitution in the LDP value, *tert*-butoxide for 1-adamantoxide.

(45) Calculated using Year 2009 single-, double-, and triple-bond covalent radii from a private communication. (a) http://www.chem.helsinki.fi/~pyykko/ (b) Pyykkö, P.; Atsumi, M. *Chem.—Eur. J.* **2009**, *15*, 12770.

(46) The average $Ti-NMe_2$ bond in CSD version 5.32 Nov 2010 is 1.897 Å. It should be noted, however, that the majority of those complexes are Ti(IV), and the distance in titanium(III) Me(H) $NTiCp^*_2$ may be somewhat longer just because of the difference in oxidation state. There are a few $Ti-NH_2$ cyclopentadienyl complexes in the CSD database, which should allow the Ti−N bond to shorten if electronically favorable. These do tend to have slightly shorter titanium-amido bond distances. For example, amidobis[1,3-bis(trimethylsilyl)cyclopentadienyl]titanium(III) has a $Ti-NH_2$ distance of 1.933(3) Å. (a) Sofield, C. D.; Walter, M. D.; Andersen, R. A. *Acta Crystallogr., Sect. C* **2004**, *60*, M465. The compound $H_2NTiCp^*_2$ has a Ti−N distance of 1.944(2) Å. (b) Brady, E.; Telford, J. R.; Mitchell, G.; Lukens, W. *Acta Crystallogr., Sect C* **1995**, *51*, 558. Neitherof these NH_2 complexes has a statistically significantdifference in the Ti−N distance from the value in $Me(H)NTiCp^*_2$, however.

(47) The methyl group isrotated in the $Me(H)N-TiCp^*_2$ complex so that theamido methyl is directed at one of the Cp* ligands. The Solid-G programcalculates the G(gamma) value to be 3.03 in this compound, which isa measure of how much of the sphere is shielded by more than one ligand.For the complex $Me(Ph)N-TiCp^*_2$, were the amido methyland phenyl groups rest between the Cp*s, the G(gamma) value is 2.19,suggesting there is less ligand overlap. In other words, the smallamido is nesting with the methyls of the Cp* groups to reach thiselectronically preferred but sterically encumbered position. For thestructure of $Me(Ph)NTiCp^*_2$ see: Feldman, J.; Calabrese, J. C. *Chem. Commun.* **1991**, 1042.

(48) For examples see: (a) Basolo, F.; Pearson, R. G. *Mechanisms of Inorganic Reactions*, 2nd ed.; Wiley & Sons: New York, 1967. (b) Burdett, J. K. *Adv. Inorg. Chem. Radiochem.* **1978**, *21*, 113. (c) Jordan, R. B. *Reaction Mechanisms of Inorganic and Organometallic Systems*, 2nd ed.; Oxford University Press: New York, 1998.